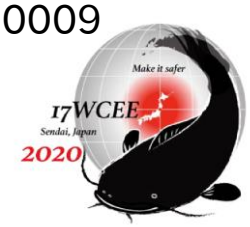

17th World Conference on Earthquake Engineering, 17WCEE
Sendai, Japan - September 13th to 18th 2020

CONNECTION BETWEEN STEEL BRACING AND CORNER JOINT USING POST-INSTALLED ANCHOR – NUMERICAL INVESTIGATION

E.J. Stehle[(1)], A. Sharma[(2)]

[(1)] *Research Associate and PhD student, Institute of Construction Materials, University of Stuttgart, erik.stehle@iwb.uni-stuttgart.de*
[(2)] *Junior Professor, Institute of Construction Materials, University of Stuttgart, Akanshu.sharma@iwb.uni-stuttgart.de*

Abstract

Reinforced concrete (RC) frame structures designed before the introduction of modern seismic codes are particularly susceptible to seismic events. The risk of a complete collapse during an earthquake and the related damage caused due to such disasters can be significantly reduced by retrofitting the RC frame structures. Hence, different methods have been developed to improve the seismic performance of the structure. One efficient and popular way is to strengthen the frame structure with steel bracings. In particular, steel bracings are very effective in remedying the soft-story mechanism. Typically, the steel braces are indirectly connected to the RC frame by means of an additional steel frame. However, this type of connection is deemed rather invasive and causes a significant increase in the weight of the structure. A preferable method is to connect the steel braces directly to the corner joints by means of post-installed anchors, offering a less invasive solution.

Nevertheless, this direct solution comes with some challenges for the connection. Due to the seismic actions high tension and shear demands are imposed on the connection and based on the column and beam dimensions the area to develop a concrete cone and the depth to transfer the bond is limited. Currently, no standard or guideline offers a design solution for these kinds of connections.

In this work such a direct connection is studied numerically and it is investigated what influence the aforementioned demands have on the performance of the retrofit solution. The numerical investigations are performed within the framework of 3D FE analysis utilizing microplane model with relaxed kinematic constraint as the constitutive law for concrete. The sub-assembly investigated includes a L-shaped reinforced concrete sub-assembly simulating the frame corner, a steel bracket connecting using post-installed bonded anchors and a simulated bracing element for application of the force.

The numerical model consists of concrete modeled using solid elements, internal reinforcement modeled using 2-node bar elements with tri-linear uniaxial stress-strain relationship, bonded anchors modeled using solid hexahedral elements with linear elastic behavior, mortar modeled using special bond elements with assigned bond stress-slip relationship according to mortar behavior, steel components modeled using solid tetrahedral or hexahedral elements with linear elastic behavior and the contact between steel and concrete modeled using compression-only contact elements. The loading is performed under displacement control until failure. The results are evaluated in terms of load-displacement behavior, crack patterns (damage) inside the concrete and the stress-transfer mechanism. The simulations form the basis of a test program which will be pursued by the authors in near future.

Keywords: seismic strengthening; post-installed anchors; steel bracing; corner joint; numerical simulation

1. Introduction

In order to overcome the structural deficiencies of reinforced concrete (RC) frames, designed before the introduction of modern seismic codes, a variety of strengthening solutions have been developed in the past decades [1]. In principal, these solutions can be classified in two categories, namely local strengthening solutions and global strengthening solutions. While local strengthening approaches, such as steel jacketing, concrete jacketing or FRP wrapping, mainly focus on the strengthening of individual elements of the structure and hence only alter the global structural behavior in terms of ductility, global strengthening solutions aim on modifying the load transfer mechanism of the structure, leading to increased global strength, stiffness and ductility characteristics. Besides the addition of shear walls, steel bracings have become a popular way to strengthen already existing buildings because of their advantages regarding flexibility, low-invasiveness, easy installation process and their beneficial effect on the global ductile behavior of the structure. Apart from the aforementioned advantages, steel bracings have proven to be an effective way to strengthen RC structures against earthquake loads by significantly increasing the lateral capacity [2, 3]. As shown by [4, 5], especially non-seismically detailed RC frame structures are prone to lateral earthquake loads. By adding steel bracings to the primary RC frame structure the load transfer mechanism changes from a moment resisting frame to a truss mechanism, resulting in improved global strength and stiffness characteristics due to the higher axial capacity and stiffness of RC frame members compared to the flexural capacity and stiffness. The development of buckling restrained braces (BRB) lead to a further improvement of the global hysteretic behavior and the ductility of the strengthened RC frame structure [6].

In order to establish the connection between the existing primary structure and the new structural steel bracing, two basic approaches can be employed. In the first approach an additional steel frame is fixed to the existing RC frame using post-installed anchors or reinforcing bars. The steel bracings are then attached to the steel frame [7, 8]. This indirect approach comes with several shortcomings. Due to the additional steel frame, the weight of the structure is significantly increased. Furthermore, the additional steel frame must be fixed to the RC frame along the complete circumference due to a lack of design guidelines. In this way the invasiveness of the solution is eminently increased and the installation process becomes rather elaborate. It becomes apparent that directly connecting the steel bracing to the primary structure offers a preferable choice, resulting in a less invasive system and minimizing the disadvantages. Several techniques for direct connections have been investigated, using steel-jackets, bolted-through connections, external rods or precast headed studs and studies [9, 10, 11, 12] have shown the feasibility and effectiveness of such direct connections. However, when it comes to the retrofit of already existing structures, these techniques are either not applicable, as in case of precast headed studs, or a two-sided access is required, which might not always be the case for existing buildings, rendering these solutions as rather unpractical. A promising alternative is the use of post-installed anchors. By using post-installed anchors to form the connection, the invasiveness is further decreased and due to the easy and comparatively fast installation process, the disturbance in the operability of the building is reduced. Experimental tests have shown that direct connections, using post-installed anchors are a feasible solution resulting in a significant increase in the global strength and energy dissipation [13, 14].

In general, the steel bracings are connected to the corner joint as for example in the experiment conducted by [14]. Therefore, the connection faces several challenges as shown in Fig.1. Due to the seismic actions high tension and shear demands are simultaneously imposed on the connection. Since the anchorage is placed close to plastic hinge zones, the anchors will inevitable be intercepted by cracks. The limited dimensions of the RC elements (like columns and beams) inhibit the development of a full concrete cone and furthermore the depth to transfer the bond is restricted. In addition, no design solution is provided by current standards or guidelines for the perpendicular arrangement of the close neighboring anchor groups in the corner joint. These challenges apply not only to the connection of steel bracings to the RC frame but they apply to most of the strengthening solutions where some kind of anchorage is needed to form the connection, like for example the attachment of haunch elements using post-installed anchors as presented in [15].

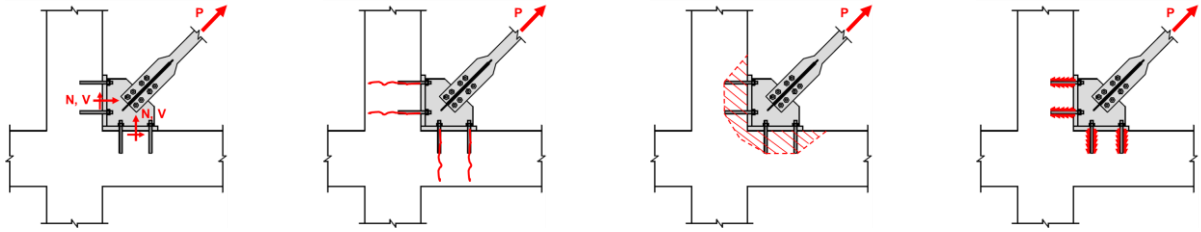

Fig. 1 – Challenges of direct connections (a) combined tension and shear load, (b) cracked concrete (c) influence of neighboring anchor group and (d) limited dimensions

Besides the specified challenges, experiments using post-installed anchors to directly connect the strengthening to the primary structure have shown that the success of the strengthening solution highly depends on the performance of the connection itself [14, 15]. Therefore, such a direct corner joint connection is studied in this work using numerical simulation. The investigated sub-assembly comprises a L-shaped concrete sub-assembly simulating the frame corner, a steel bracket connection using post-installed bonded anchors and a gusset plate for the application of the forces. In the 3D FE analysis, the microplane model with relaxed kinematic constraint is deployed as the constitutive law for concrete. Steel is modelled as linear elastic, since concrete failure is expected before yielding of the steel parts. The aim of the numerical analysis is to gain a better understanding of this type of direct connections and to investigate the influence of the aforementioned demands and challenges on the performance of the retrofit solution. A particular emphasis is on the influence of the neighboring anchor groups regarding the concrete breakout behavior. The numerical simulation forms the basis for an experimental test program which will be pursued by the authors in the near future.

2. Numerical simulation

2.1 The finite element code MASA

The numerical analysis is performed using the 3D FE software MASA, developed at the Institute of Construction Materials, University of Stuttgart. The main application of MASA is the nonlinear analysis of concrete and RC structures, thereby damage and fracture phenomena are treated by means of a smeared crack approach. The constitutive law for concrete is based on the microplane model with relaxed kinematic constraint proposed by [16]. In this model the material is characterized by a relation between the stress and the strain components on planes of various orientations. These planes can be interpreted as the damage planes or weak planes at a microstructural level. In respect of concrete this means, that the planes can be seen as the contact layers between the aggregates. Every microplane is able to resist normal and shear strain components (ε_N, ε_T) as illustrated in Fig.2. In order to realistically model concrete for dominant compressive load and to control the initial elastic value of the Poisson's ratio, the normal strain component ε_N is decomposed in a volumetric (ε_V) and a deviatoric (ε_D) part. This decomposition results in a pathological behavior when it comes to dominant tensile load, which leads to lateral expansion when subjected to uniaxial tension load. Therefore, the microplane strain components are modified in a way that relaxes the kinematic constraint. In MASA, kinematic constraint replaces the static constraint in order to provide the uniqueness of the solution for softening (quasi-brittle) materials such as concrete. This is achieved by calculating the microplane strain components as the projection of the macroscopic strain tensor.

In the FE analysis using a classical local smeared crack approach for materials which exhibit softening such as concrete (quasi-brittle materials), the results can be mesh dependent [17]. The reason for this phenomenon is the localization of damage and related energy consumption capacity which depends on the

element size. In case of coarse finite element meshes (rather large element size) the energy consumption capacity will be larger and the ultimate load higher than if the mesh is fine (rather small element size). Hence, the model response is mesh dependent. To ensure a mesh independent model response, the total energy consumption capacity has to be independent of the element size. This can be achieved by implementing so-called localization limiter. In MASA the crack band method is implemented to achieve size independent results. Hereby the damage (crack) is localized in a row of finite elements and the constitutive law for concrete is modified in way to ensure constant and mesh independent energy consumption capacity of concrete.

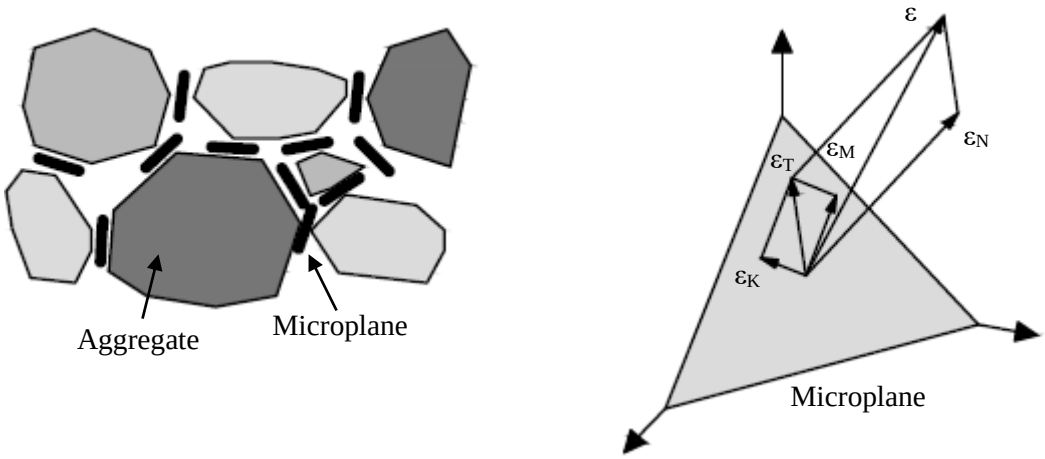

Fig. 2 – Microplane model (a) idealization of contact layers between aggregates and (b) decomposition of the total macroscopic strain tensor

In this work the main emphasis is on the behavior of the connection in case of concrete failure. Hence concrete failure is expected before the yielding of the steel components (anchor rods, anchor bracket and gusset plate). In this case steel nonlinearity can be neglected and a linear-elastic material behavior is assumed for all steel components.

For pre- and post-processing, the software FEMAP is utilized. In FEMAP the nodes, elements, boundary conditions, material data and loads are generated. Through an input interface program, the FEMAP output data is converted into the input data for the FE code. Through an output interface program, the numerical results of the FE analysis are in turn converted into post-processing output results which can be read and graphically interpreted by FEMAP [17].

2.2 Numerical model

To simulate the frame corner joint, a L-shaped concrete specimen was modeled, using the same dimensions for the beam and column elements. The exact dimensions of the concrete specimen are given in Fig.3. The concrete specimen is unreinforced in order to prevent any influence on the concrete breakout behavior. Further it serves as the base material for the anchorage which is placed in the corner of the L-shaped specimen. The anchorage comprises a bracket connection using 12 bonded anchors to fasten the anchor bracket to the concrete specimen. The dimension of the anchor bracket is given in Fig.3. The anchor rods were modelled with a diameter d_s = 16 mm and were embedded in the concrete with an effective embedment depth of h_{ef} = 100 mm. The spacing between the anchors is s_1 = 100 mm and s_2 = 160 mm. The anchors are placed close to the edges of the beam and column elements with an edge distance of c_2 = 70 mm. To simulate the bracing element and to apply the forces, a gusset plate with a thickness of 25 mm was modelled as shown in Fig.3. The discretization of the concrete specimen and the steel components is shown in Fig.4. 8-node solid hexahedral elements are used to model the anchor rods, the anchor bracket and the gusset plate. To

model the concrete, 4-node solid tetrahedral elements are used. The bond between steel and concrete is modelled using 2-node bar elements with assigned bond stress-slip relationship according to mortar behavior. These elements are able to transfer compression and shear forces. To model the contact between steel and concrete, compression only contact elements are utilized.

The load is directly applied to the nodes in terms of displacement in the middle of the inclined side face of the gusset plate as indicated in Fig.4(a). The load is evenly applied in the x- and z-direction, so the resultant direction of the load is at an angle of 45° to the x- and z-axis. The load is stepwise increased in displacement increments of 0.01 mm. To calculate the total force, the sum of forces on the loaded nodes in the direction of the applied displacement is taken. To represent experimental support conditions, additional steel plates are modelled at the column- and beam-end faces in order to confine the specimen. The constraints are directly applied to the nodes in the respective direction of the beam/column.

The material properties for steel and concrete are given in Table 1. It is worth to mention that the microplane model parameters are generated automatically from the basic macroscopic concrete properties as given in Table 1. The concrete properties correspond to the concrete strength class C20/25. As already mentioned, steel is only considered as linear-elastic and therefore the only material properties that have to be defined are Young's modulus and Poisson's ratio.

The applied modelling approach has been utilized in previous studies [18, 19]. In these studies, it was demonstrated that this approach is capable of realistically capture the behavior of concrete when used as the base material for multiple-anchor connections.

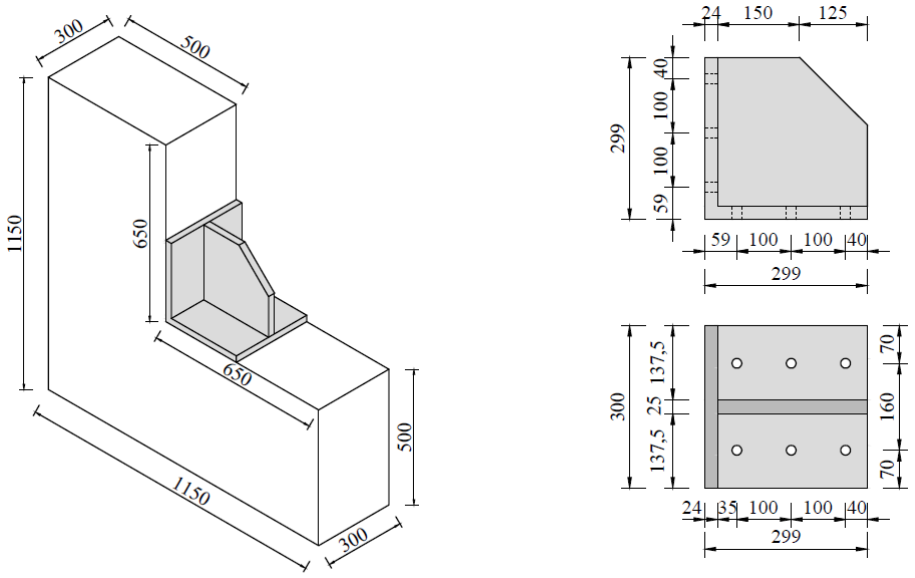

(a) (b)

Fig. 3 – Dimensions (in mm) of (a) the concrete specimen and (b) the anchor bracket and gusset plate connection

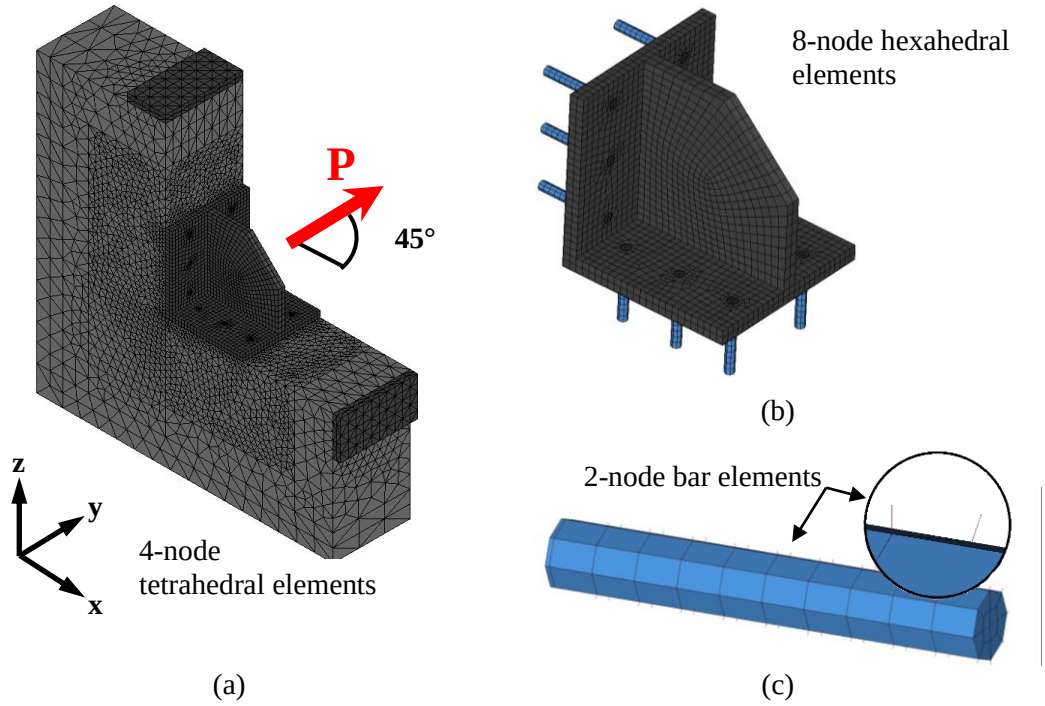

Fig. 4 – Discretization (a) complete FE model, (b) anchor bracket, gusset plate and anchor rods and (c) anchor rod with 2-node bar elements for bond

Table 1 – Material properties for steel and concrete

Material	Young's modulus, E (N/mm²)	Poisson's ratio, ν (-)	Tensile strength, f_t (N/mm²)	Compressive strength, f_c (N/mm²)	Fracture energy, G_f (N/mm)
Concrete	30000	0.18	2.20	20.00	0.07
Steel	200000	0.33	-	-	-

3. Numerical results

3.1 Load-displacement behavior

In this section the results of the numerical analysis are presented. Fig.5 depicts the load-displacement curve obtained from the numerical analysis and Fig.6 illustrates the progression of secant stiffness along with the displacement of the connection. The load refers to the total force P which is taken as the sum of forces on the loaded nodes in the direction of the applied displacement. The displacement refers to the applied resultant displacement at the inclined side face of the gusset plate. The ultimate load of the connection is P_u = 399 kN and the corresponding displacement is s_u = 0.665 mm. As can be seen, the behavior of the connection is almost linear until it reaches the ultimate load. This is also reflected by comparing the secant stiffness at 0.5 P_u and P_u. At 0.5 P_u, the secant stiffness is calculated as $K_{0.5Nu}$ = 794 kN/mm and at P_u the secant stiffness is calculated as K_{Nu} = 600 kN/mm. After reaching ultimate load, the load drops rather fast in the ascending branch up to a load of P = 364 kN at 0.863 mm displacement. Also, from Fig.6 it can be seen, that the stiffness undergoes a sudden drop after reaching ultimate load. Thereafter the load slightly increases again until the second peak at 375 kN. The corresponding displacement is 1.188 mm. After the second peak, the load decreases further. At 2.432 mm displacement, 80% of the ultimate capacity in the post-peak range is reached.

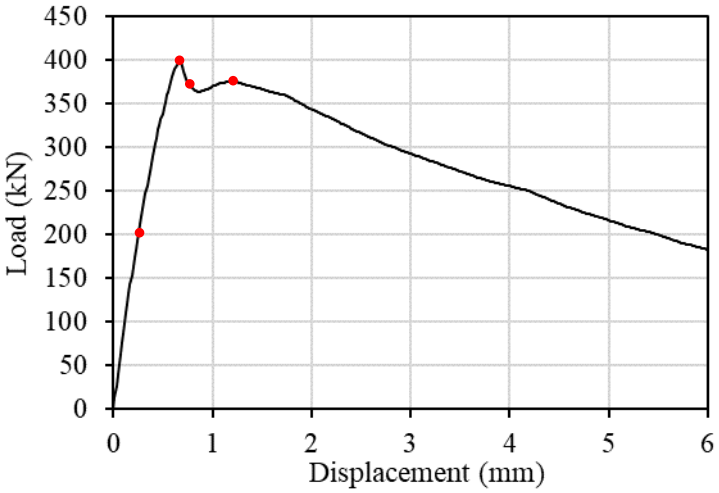

Fig. 5 – Load-displacement curve obtained from the numerical analysis

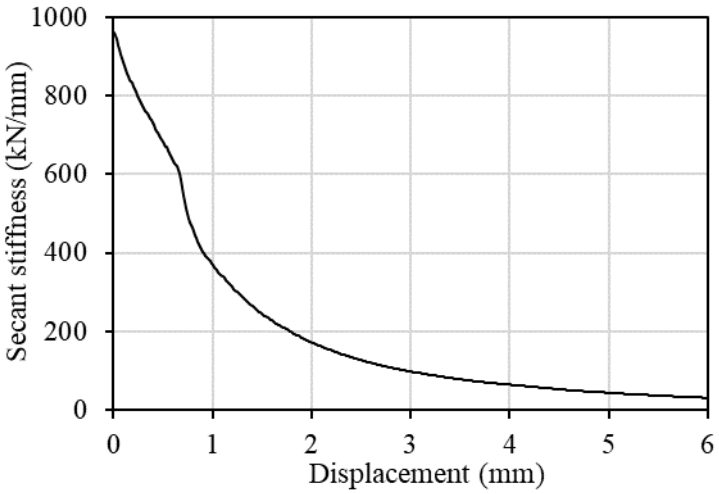

Fig. 6 – Progression of secant stiffness over the displacement of the connection

3.2 Crack pattern

While during an experiment the damage happening inside the concrete cannot be investigated, numerical simulations allow to assess the damage inside the concrete specimen regarding the crack pattern and the crack propagation. Fig.7 shows the crack patterns obtained from the numerical analysis of the corner joint connection. On the left side, the 3D view is illustrated showing the crack pattern on the surface of the concrete specimen at different stages of loading. The right side shows the cutting section through the left anchor row (x-z-plane). The cracks are displayed in terms of principal tensile strain. Red elements represent cracks with a crack width of 0.1 mm or larger. In the following, the complete bracket connection is considered as two perpendicular 3 x 2 anchor groups. In these anchor groups, back anchors refer to the two anchors which are placed closest to the corner and front anchors refer to the two anchors which are placed farthest away from the corner. Four loading stages are shown in Fig.7. In addition, the stages are marked with a red dot on the load-displacement curve, shown in Fig.5.

At the first loading stage, at approximately 0.5 P_u, the connection is still in the linear elastic range and no cracking is observed. At ultimate load, cracks on the surface and at the tips of the embedded ends of the

anchor rods have formed between the back anchors and the anchors in the middle of the 3 x 2 anchor groups. At the bottom of the breakout body, the cracks have propagated from the tips of the embedded end of the anchor rods towards each other and form a horizontal crack when they merge. Miner cracks have also started propagating from the middle anchors towards the front anchors. At ultimate load the cracks have not yet propagated to the surface of the side faces of the concrete specimen. By loading the connection beyond ultimate load, cracks also form between the middle anchors and the front anchors. At the bottom of the concrete breakout body horizontal cracks have formed between the tips of the anchor rods, which are in general wider than the cracks observed at the surface. Furthermore, cracks start to propagate between the two back anchors and from the back anchors towards the edges of the concrete specimen. From the embedded ends of the back anchors of the two perpendicular groups, cracks start to propagate towards each other. The cracks result from the compression strut forming between the back anchors of the groups. In general, when the concrete cone can form without restrictions, the slope of the concrete breakout body and the surface is approximately 35° as shown in [20]. Different from that, the slope of the crack between the back anchors of the groups is 45°, due to the geometric conditions of the connection. Also, cracks propagate towards the surface of the side faces of the specimen and form visible cracks at the surface. At the second peak of the load-displacement curve, the cracks propagating from the back anchors of the two groups towards each other have merged and form a single crack. At the same time, a second cone appears to be forming from the back anchors.

4. Conclusion

In this work, a L-shaped concrete sub-assembly simulating a frame corner was investigated numerically. An anchor bracket and gusset plate connection was attached to the frame corner using bonded anchors, to simulate the connection between a steel bracing element and the frame structure. The objective of the study was to assess the load-displacement behavior of such a connection, facing various challenges like close edges, high combined tension and shear loads and the effect of the perpendicular arrangement of close neighboring anchor groups. Due to the numerical analysis, the damage process in the anchorage material in terms of cracking could be investigated. Based on the numerical results, the following conclusions can be drawn:

1. Before failure, the connection was able to withstand a load of almost 400 kN at a displacement of 0.665 mm. Until the point of ultimate load, the connection behaves relatively stiff, with a linear degradation of the secant stiffness. Upon reaching ultimate load, a significant drop in the secant stiffness was observed.
2. While loading until ultimate load, the two perpendicular anchor groups of the connection seem to have no notable influence on each other. Cracking starts at the embedded ends of the back anchors and the middle anchors. This indicates, that at first the back anchors get more load, which is than distributed to the front anchors.
3. The influence of the two groups becomes apparent when a compression strut forms between the back anchors of the two groups and a crack with a slope of 45° propagates between the embedded ends of these anchors towards each other. Due to the perpendicular anchor groups, the slope of the crack is steeper than in case of an unrestricted concrete cone breakout body.
4. Cracks forming from the back anchors towards the edges of the concrete specimen indicate the negative influence of the close edges on the anchors.

The numerical results form the basis of a test program which will be pursued by the authors in the near future.

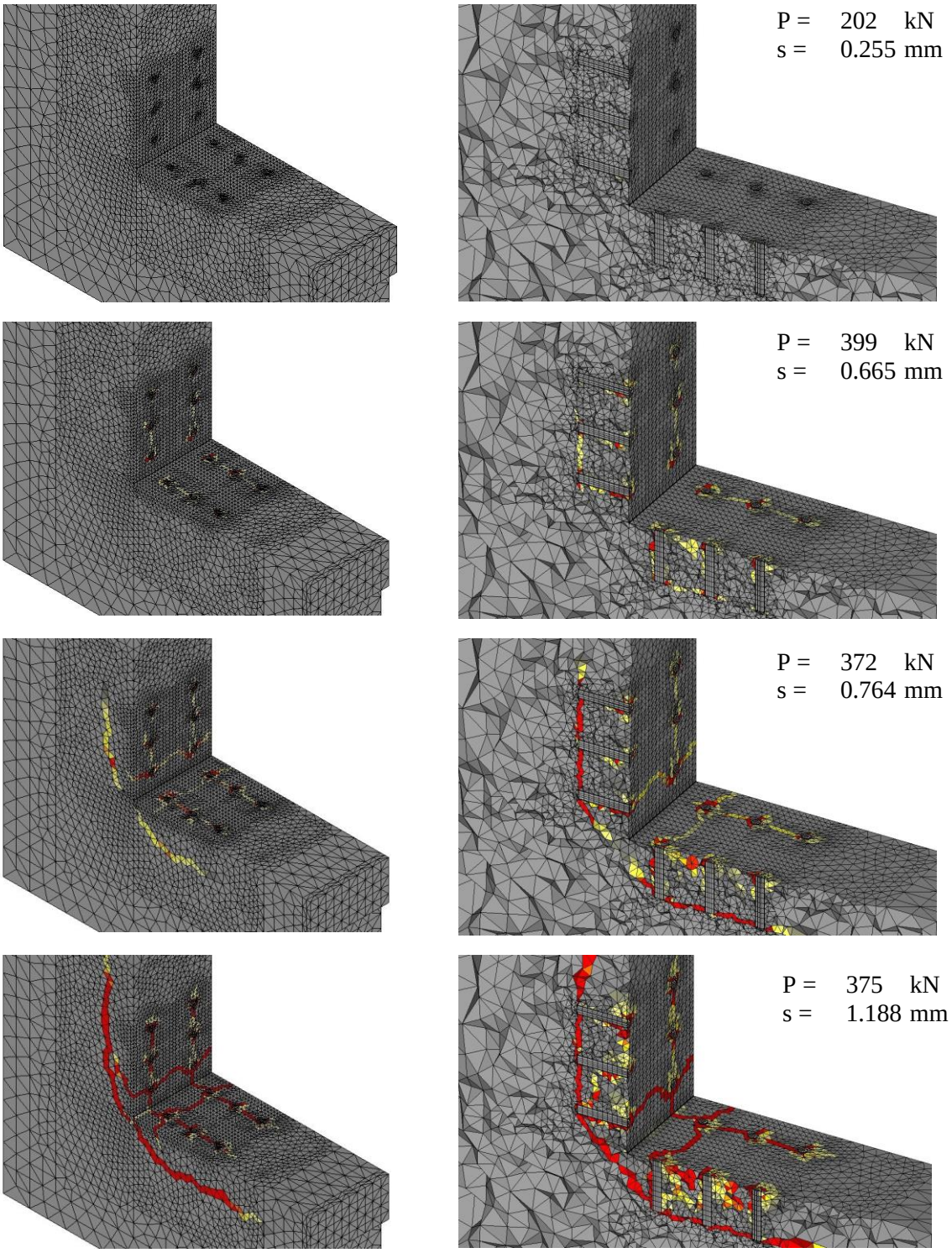

(a) 3D view (b) Section cut

Fig. 7 – Crack pattern for various loading stages

5. Acknowledgements

The authors wish to thank fischerwerke GmbH & Co. KG. The support provided by fischerwerke is greatly acknowledged. Opinions, conclusions, and recommendations expressed in this paper are those of the authors and do not necessarily reflect those of the sponsoring organization.

6. References

[1] Sugano S (1996): State-of-the-art in techniques for rehabilitation of buildings. *11th World Conference on Earthquake Engineering*, Acapulco, Mexico.

[2] Abou-Elfath H, Ghobarah A (2000): Behaviour of reinforced concrete frames rehabilitated with concentric steel bracing. *Canadian Journal of Civil Engineering*, **27** (3), 433-444.

[3] Badoux M, Jirsa JO (1990): Steel bracing of RC frames for seismic retrofitting. *Journal of Structural Engineering*, **116** (1), 55-74.

[4] Liel AB, Haselton CB, Deierlein GG (2011): Seismic collapse safety of reinforced concrete buildings. II: Comparative assessment of nonductile and ductile moment frames. *Journal of Structural Engineering*, **137** (4), 492-502.

[5] Sadjadi R, Kianoush MR, Talebi S (2007): Seismic performance of reinforced concrete moment resisting frames. *Engineering Structures*, **29** (9), 2365-2380.

[6] Watanabe A, Hitomi Y, Saeki E, Wada A, Fujimoto M (1988): Properties of brace encased in buckling-restraining concrete and steel tube. *9th World Conference on Earthquake Engineering*, Tokyo-Kyoto, Japan.

[7] Usami H, Azuchi T, Kamiya Y, Ban H, Kenjo H, Suzuki U (1988): Seismic strengthening of existing reinforced concrete buildings in Shizuoka prefecture, Japan. *9th World Conference on Earthquake Engineering*, Tokyo-Kyoto, Japan.

[8] Ohishi H, Takahashi M, Yamazaki Y (1988): A seismic strengthening design and practice of an existing reinforced concrete school building in Shizuoka city. *9th World Conference on Earthquake Engineering*, Tokyo-Kyoto, Japan.

[9] Maheri MR, Hadjipour A (2003): Experimental investigation and design of steel brace connection to RC frame. *Engineering Structures*, **25** (13), 1707-1714.

[10] Massumi A, Tasnimi AA (2008): Strengthening of low ductile reinforced concrete frames using steel X-bracings with different details. *14th World Conference on Earthquake Engineering*, Beijing, China.

[11] TahamouliRoudsari M, Entezari A, Hadidi M, Gandomian O (2017): Experimental assessment of retrofitted RC frames with different steel braces. *Structures*, **11**, 206-217.

[12] Maheri MR, Ghaffarzadeh H (2006): Internal steel bracing for seismic design of RC buildings. *8th International Conference on Steel & Space Structures*, Kuala Lumpur, Malaysia.

[13] Yooprasertchai E, Warnitchai P (2008): Seismic retrofitting of low-rise nonductile reinforced concrete buildings by buckling-restrained braces. *14th World Conference on Earthquake Engineering*, Beijing, China.

[14] Mahrenholtz C, Lin P-C, Wu A-C, Tsai K-C, Hwang S-J, Lin R-Y, Bhayusukma MY (2015): Retrofit of reinforced concrete frames with buckling-restrained braces. *Earthquake Engineering & Structural Dynamics*, **44** (1), 59-78.

[15] Sharma A (2013): Seismic behavior and retrofitting of RC frame structures with emphasis on beam-column joints – experiments and numerical modeling. *PhD Thesis*, University of Stuttgart, Germany.

[16] Ožbolt J, Li Y, Kožar I (2001): Microplane model for concrete with relaxed kinematic constraint. *International Journal of Solids and Structures*, **38** (16), 2683-2711.

[17] Ožbolt J: MASA: Finite element program for 3D nonlinear analysis of concrete and reinforced concrete structures. *Manual*, Institute of Construction Materials, University of Stuttgart, Germany.

[18] Stehle EJ, Sharma A (2019): Numerical investigation of anchor groups under seismic tension actions. *Otto Graf Journal*, **18**, 313-324.

[19] Grosser PR (2012): Load-bearing behavior and design of anchorages subjected to shear and torsion loading in uncracked concrete. *PhD Thesis*, University of Stuttgart, Germany.

[20] Eligehausen R, Mallee R, Silva JF (2006): *Anchorage in Concrete Construction*. Berlin: Ernst & Sohn, Germany.

